

Dynamical collapse in a degenerate binary fermion mixture using a hydrodynamic model

Sadhan K. Adhikari[‡]

Instituto de Física Teórica, UNESP – São Paulo State University, 01.405-900 São Paulo, São Paulo, Brazil

Abstract.

We use a time-dependent dynamical hydrodynamic model to study a collapse in a degenerate fermion-fermion mixture (DFFM) of different atoms. Due to a strong Pauli-blocking repulsion among identical spin-polarized fermions at short distances there cannot be a collapse for repulsive interspecies fermion-fermion interaction. However, there can be a collapse for a sufficiently attractive interspecies fermion-fermion interaction in a DFFM of different atoms. Using a variational analysis and numerical solution of the hydrodynamic model we study different aspects of collapse in such a DFFM initiated by a jump in the interspecies fermion-fermion interaction (scattering length) to a large negative (attractive) value using a Feshbach resonance. Suggestion for experiments of collapse in a DFFM of distinct atoms is made.

PACS numbers: 03.75.Ss

[‡] Electronic address: adhikari@ift.unesp.br;
URL: <http://www.ift.unesp.br/users/adhikari/>

1. Introduction

Recent successful observation of degenerate boson-fermion mixture (DBFM) and fermion-fermion mixture (DFFM) of trapped alkali-metal atoms by different experimental groups [1–7] has initiated the intensive experimental studies of different novel phenomena [8–10]. It has been possible to achieve a degenerate Fermi gas (DFG) by sympathetic cooling in the presence of a second boson or fermion component, as there cannot be an effective evaporative cooling [1] of a single-component DFG due to a strong Pauli-blocking repulsion at low temperature among spin-polarized fermions. Among these experiments on a DFG, apart from the study of a DBFM in ${}^6,{}^7\text{Li}$ [6], ${}^{23}\text{Na}-{}^6\text{Li}$ [7] and ${}^{87}\text{Rb}-{}^{40}\text{K}$ [9–12], there have been studies of a DFFM in ${}^{40}\text{K}-{}^{40}\text{K}^*$ [1] and ${}^6\text{Li}-{}^6\text{Li}^*$ [2–5] systems, where $*$ denotes a distinct hyperfine state. More recently the formation of a Bardeen-Cooper-Schreiffer (BCS) condensate of fermionic ${}^6\text{Li}$ atoms in ${}^{23}\text{Na}-{}^6\text{Li}$ [13] and ${}^6\text{Li}-{}^6\text{Li}^*$ [4] mixtures has been observed experimentally. The collapse in a DBFM of ${}^{87}\text{Rb}-{}^{40}\text{K}$ atoms has been observed and studied by Modugno *et al.* [9] and more recently by Ospelkaus *et al.* [11]. Recently, experiments on controlled collapse on ${}^{87}\text{Rb}-{}^{40}\text{K}$ have been accomplished [14].

A collapse in a Bose-Einstein condensate (BEC) takes place due to an attractive atomic interaction [15, 16]. A study of controlled collapse and explosion has been performed by Donley *et al.* [16] on an attractive ${}^{85}\text{Rb}$ BEC, where they manipulated the inter-atomic interaction by varying a background magnetic field exploiting a nearby Feshbach resonance [17]. There have been many theoretical [18, 19] studies to describe different features of this experiment [16]. More recently, there have been experimental studies on collapse in a DBFM of ${}^{87}\text{Rb}-{}^{40}\text{K}$ by two different groups [9, 11, 14] as well as related theoretical investigations [20, 21]. As the interaction in a pure DFG at short distances is repulsive due to Pauli-blocking, there cannot be a collapse in it. The Pauli repulsion is responsible for the stability of a neutron star against a (gravitational) collapse. A collapse is possible in a DBFM in the presence of a sufficiently strong boson-fermion attraction which can overcome the Pauli repulsion among identical fermions [9, 11, 20].

In this paper we study the collapse in a DFFM for a sufficiently attractive interspecies fermion-fermion interaction which can overcome the Pauli repulsion. However, there is already experimental evidence and theoretical conjecture that a Fermi gas in two (spin) hyperfine states of the same atom is much more stable [22] than expected on the basis of a scattering length approach [5, 23] and there is no collapse in such a system. A similar conclusion follows from an examination of the compressibility of such a system [24]. A strongly attractive DFFM in two (spin) hyperfine states exhibits universal behavior and should be mechanically stable as a consequence of the quantum-mechanical requirement of unitarity. This requirement limits the maximum attractive force for such a DFFM to a value smaller than that of the outward Fermi pressure due to Pauli repulsion [22]. It has been demonstrated that a two-component DFFM in different (spin) hyperfine states is stable against collapse [25], whereas a multicomponent

degenerate fermion mixture [22, 25] or a DFFM of different atoms [26] could undergo collapse. Hence, by taking a DFFM of two different fermionic atoms of different atomic mass one can avoid the problem [22, 25] of a possible suppression of collapse. Thus one could study collapse in a DFFM in the same manner as in a DBFM. The second component of fermions will then only aid in inducing an attraction among the fermions of the first component responsible for collapse without suppressing the collapse. Although, the past experiment [22] on two-component cold Fermi gas used two (spin) hyperfine states of the same atom, experiments can be realized with distinct atoms and one can look for collapse in such a system. One such system is the ${}^6\text{Li}$ - ${}^{40}\text{K}$ mixture: both ${}^6\text{Li}$ [4] and ${}^{40}\text{K}$ [1] have been trapped and studied in laboratory.

Here we use a coupled time-dependent mean-field hydrodynamic model which is inspired by the success of a similar model used by the present author in the investigation of a fermionic collapse [20] and bright [27] and dark [28] solitons in a DBFM as well as of mixing-demixing [29] and black solitons [30] in a DFFM. The conclusions of the study on bright soliton [27] are in agreement with a microscopic study [31] and the noted survival of collapse in the numerical study [20] has been experimentally substantiated later in a DBFM of ${}^{40}\text{K}$ - ${}^{87}\text{Rb}$ [11]. A very similar model has been used by Jezek *et al.* [32] in a successful description of vortex states in a DBFM. Although, a mean-field model is simple to use and leads to a proper prediction of probability density of the fermionic system, many true quantum effects are lost in this simplified model, e. g., it cannot predict the suppression of collapse of a DFFM in two different (spin) hyperfine states [22, 25] as discussed in the last paragraph. We recall many true quantum effects are also lost [33] in the mean-field Gross-Pitaevskii equation for trapped bosons.

In our study on collapse in a DFFM we shall consider a strong attraction among fermions which will naturally lead to molecule formation and not to a BCS state. A BCS state is usually formed for a weak attraction among identical fermions. The possibility of molecule formation by three-body recombination is explicitly included in our model by an absorptive nonlinear term. Apart from the direct experimental interest in trapped cold atoms, a study of strongly interacting Fermi gases and their possible collapse is also relevant [22] in condensed matter physics (superconductivity), nuclear physics (nuclear matter), high energy physics (effective theories of strong interaction), and astrophysics (compact stellar objects), which makes the present study of greater interest.

The collapse in a DFFM is first studied by a variational analysis of the present model, which is later substantiated by a complete numerical solution using the Crank-Nicholson scheme [34]. During a collapse and an explosion of the DFFM, the system loses atoms as in a collapsing and exploding BEC [16]. The loss of atoms is accounted for by three-body recombination involving two types of fermions. We study the sensitivity of our results on the three-body recombination loss rates. We also study the quasi-periodic oscillation of the sizes of the DFFM undergoing a collapse. The collapse is to be initiated by jumping the interspecies scattering length to a large negative (attractive) value near a fermion-fermion Feshbach resonance [35]. However, the collapse starts after a time delay upon this jump and we study the variation of this time delay with the final

scattering length. This variation has a behavior similar to that observed in the bosonic case [16]. The collapsing DFFM is found to execute a quasi-periodic oscillation with a frequency approximately equal to twice the frequency of the harmonic trap as in a BEC [16].

Previously, in addition to the study of a collapse in a pure BEC [18, 19], we also investigated [36] the collapse in a two-species BEC initiated by an interspecies attraction. The predicted collapse in a two-species BEC for intra-species repulsion and interspecies attraction [36] is similar to that in a DBFM of ^{87}Rb - ^{40}K studied before [9, 11, 20] and that in a DFFM studied in this paper.

In section 2 we present the coupled hydrodynamic model for a DFFM which we apply to predict and study a collapse. In this section we also present a variational analysis based on this model which substantiates the collapse in a DFFM for a sufficiently attractive interspecies fermion-fermion attraction. In section 3 we present results of numerical simulation of our study on collapse. Finally, in section 4 we present a brief summary of our investigation.

2. Coupled Hydrodynamic Model for a Fermion-Fermion Mixture

2.1. Model

A mean-field-hydrodynamic Lagrangian for a DFG has been used successfully in the study of a DBFM [27, 28, 32] which we shall use in the present investigation. The virtue of the hydrodynamic model for a DFG over a microscopic description is its simplicity and good predictive power. To develop a set of practical time-dependent hydrodynamic equations for a DFFM, we consider the following Lagrangian density [27, 28]

$$\begin{aligned} \mathcal{L} &= \frac{i}{2}\hbar \sum_{j=1,2} \left(\Psi_j \frac{\partial \Psi_j^*}{\partial t} - \Psi_j^* \frac{\partial \Psi_j}{\partial t} \right) \\ &+ \sum_{j=1}^2 \left(\frac{\hbar^2 |\nabla \Psi_j|^2}{6m_j} + V_j n_j + \frac{3}{5} A_j |n_j|^{5/3} \right) \\ &+ g_{12} n_1 n_2 - i\hbar (K_{31} n_1 n_2^2 + K_{32} n_1^2 n_2), \end{aligned} \quad (2.1)$$

where m_j is the mass of component j ($= 1, 2$), $A_j = \hbar^2(6\pi^2)^{2/3}/(2m_j)$, Ψ_j is a complex probability amplitude, $n_j = |\Psi_j|^2$ is a real probability density and $N_j \equiv \int d\mathbf{r} n_j(\mathbf{r})$ the number. Here the interspecies coupling is $g_{12} = 2\pi\hbar^2 a_{12}/m_R$ with the reduced mass $m_R = m_1 m_2 / (m_1 + m_2)$, and a_{12} is the interspecies scattering length. The spherically-symmetric potential is taken as $V_j(\mathbf{r}) = \frac{1}{2}(3m_j)\omega^2 r^2$ where ω is the radial (r) frequency. The interaction between intra-species fermions in spin-polarized state is highly suppressed due to Pauli blocking and has been neglected in (2.1) and will be neglected throughout. The kinetic energy terms in this equation are derived from a hydrodynamic equation for the fermions [37]. The kinetic energy terms contribute little to this problem compared to the dominating Pauli blocking term $3A_j |n_j|^{5/3}/5$ in (2.1). However, its inclusion leads to a smooth solution for the probability density

everywhere [27]. The Lagrangian density of each fermion component in (2.1) is identical to that used in Refs. [27, 28]. The last two terms in (2.1) correspond to three-body recombination due to the following reactions, respectively $F_1 + F_2 + F_2 \rightarrow (F_1 F_2) + F_2$, and $F_1 + F_2 + F_1 \rightarrow (F_1 F_2) + F_1$, where $(F_1 F_2)$ is a composite structure (resonance/molecule) of fermions F_1 and F_2 and K_{31} and K_{32} are the corresponding three-body loss rates. The contribution to the Lagrangian density of the recombination reactions is proportional to the density of the participating fermions. Here we neglected two-body loss.

The dynamical equations for the system are just the usual Euler-Lagrange (EL) equations with the Lagrangian density (2.1) [38]

$$\frac{\partial}{\partial t} \frac{\partial \mathcal{L}}{\partial \frac{\partial \Psi_j^*}{\partial t}} + \sum_{k=1}^3 \frac{d}{dx_k} \frac{\partial \mathcal{L}}{\partial \frac{\partial \Psi_j^*}{\partial x_k}} = \frac{\partial \mathcal{L}}{\partial \Psi_j^*}, \quad (2.2)$$

where $x_k, k = 1, 2, 3$ are the three space components, and $j = 1, 2$ refer to the fermion components. Consequently, the following EL equations of motion are derived:

$$\left[-i\hbar \frac{\partial}{\partial t} - \frac{\hbar^2 \nabla_{\mathbf{r}}^2}{6m_1} + V_1(\mathbf{r}) + A_1 |n_1|^{2/3} + g_{12} n_2 - i\hbar (K_{31} n_2^2 + 2K_{32} n_1 n_2) \right] \Psi_1 = 0. \quad (2.3)$$

$$\left[-i\hbar \frac{\partial}{\partial t} - \frac{\hbar^2 \nabla_{\mathbf{r}}^2}{6m_2} + V_2(\mathbf{r}) + A_2 |n_2|^{2/3} + g_{12} n_1 - i\hbar (2K_{31} n_1 n_2 + K_{32} n_1^2) \right] \Psi_2 = 0. \quad (2.4)$$

In the spherically-symmetric state the fermion density has the form $\Psi_j(\mathbf{r}; t) = \psi_j(r; t)$. Now transforming to dimensionless variables defined by $x = \sqrt{2}r/l$, $\tau = t\omega$, $l \equiv \sqrt{\hbar/(m\omega)}$, $m = 3m_1 = 3m_2$ and

$$\frac{\phi_j(x; \tau)}{x} = \sqrt{\frac{4\pi l^3}{N_j \sqrt{8}}} \psi_j(r; t), \quad (2.5)$$

we obtain from (2.3) and (2.4)

$$\left[-i \frac{\partial}{\partial \tau} - \frac{\partial^2}{\partial x^2} + \frac{x^2}{4} + \mathcal{N}_{11} \left| \frac{\phi_1}{x} \right|^{4/3} + 6\sqrt{2} \mathcal{N}_{12} \left| \frac{\phi_2}{x} \right|^2 - i2\xi_{32} \mathcal{N}_{12} \mathcal{N}_{21} \left| \frac{\phi_1}{x} \right|^2 \left| \frac{\phi_2}{x} \right|^2 - i\xi_{31} \mathcal{N}_{12}^2 \left| \frac{\phi_2}{x} \right|^4 \right] \phi_1(x; \tau) = 0, \quad (2.6)$$

$$\left[-i \frac{\partial}{\partial \tau} - \frac{\partial^2}{\partial x^2} + \frac{x^2}{4} + \mathcal{N}_{22} \left| \frac{\phi_2}{x} \right|^{4/3} + 6\sqrt{2} \mathcal{N}_{21} \left| \frac{\phi_1}{x} \right|^2 - i2\xi_{31} \mathcal{N}_{12} \mathcal{N}_{21} \left| \frac{\phi_1}{x} \right|^2 \left| \frac{\phi_2}{x} \right|^2 - i\xi_{32} \mathcal{N}_{21}^2 \left| \frac{\phi_1}{x} \right|^4 \right] \phi_2(x; \tau) = 0, \quad (2.7)$$

where $\mathcal{N}_{jj} = 3(3\pi N_j/2)^{2/3}$, $\mathcal{N}_{12} = N_2 a_{12}/l$, $\mathcal{N}_{21} = N_1 a_{12}/l$, $\xi_{32} = K_{32}/(2\pi^2 a_{12}^2 l^4 \omega)$, and $\xi_{31} = K_{31}/(2\pi^2 a_{12}^2 l^4 \omega)$. In the non-absorptive case without any loss of atoms due to three-body recombination $\xi_{31} = \xi_{32} = 0$, the normalization of the wave-function components is given by $\int_0^\infty dx |\phi_j(x; \tau)|^2 = 1$, $j = 1, 2$. In the absorptive case $\xi_{31} \neq 0$ and $\xi_{32} \neq 0$ it is possible to have loss of atoms due to three-body recombination and the normalization reduces with time due to loss of atoms.

We solve the coupled hydrodynamic equations (2.6) and (2.7) numerically using a time-iteration method based on the Crank-Nicholson discretization scheme elaborated in Refs. [34, 39]. We discretize the hydrodynamic equations using time step 0.00025 and space step 0.025 spanning x from 0 to 25. This domain of space was sufficient to encompass the entire fermion function during a collapse and explosion and obtain convergent solution for the total number of fermions. First we solve (2.6) and (2.7) with $\xi_{31} = \xi_{32} = 0$ to find an initial stationary state of the DFFM. It is true that the three-body loss, taken care of by terms ξ_{31} and ξ_{32} , is always present in the system, its effect is small leading to at best a small loss rate in atoms except for very large negative values of a_{12} . Hence, for the consideration of the initial state, we could as well neglect three-body loss. (This is why a Gross-Pitaevskii mean-field equation without three-body loss has been successfully used to study many features of a repulsive trapped BEC [33].) However, in the final state, when a_{12} is suddenly turned to a large negative value by a Feshbach resonance, the three-body loss has a dramatic effect responsible for a proper description of a collapse and explosion with a very rapid loss of atoms in a short interval of time (see figure 3).

In our numerical investigation we take $l = 1 \mu\text{m}$ and consider the equal-mass fermions with the mass of ^{40}K corresponding to a radial frequency $\omega \approx 2\pi \times 83 \text{ Hz}$. The present simplified mean-field model cannot predict the suppression of collapse [22, 25] of a DFFM in two hyperfine states which is a true quantum many-body effect. Nevertheless, it leads to a proper description of collapse dynamics of a DFFM of two distinct atoms. The use of equal-mass fermions only keeps the algebra simple specially in section 2.2, but otherwise has no effect on the general qualitative dynamics studied in this paper. In this study, the unit of time is $1/\omega \approx 2 \text{ ms}$, and unit of length $l/\sqrt{2} \approx 0.7 \mu\text{m}$. Actually, any two different fermionic atoms can be used in experiment, a proper quantitative treatment of which will require the use of different mass factors in the dynamical equations.

2.2. Variational Analysis

To understand how the stationary states of a DFFM are formed, we employ a variational method for the solution of (2.6) and (2.7) in the symmetric case $N_1 = N_2 \equiv N$, while $\phi_1/x = \phi_2/x \equiv \varphi$ satisfies

$$\left[-i \frac{\partial}{\partial \tau} - \frac{\partial^2}{\partial x^2} - \frac{2}{x} \frac{\partial}{\partial x} + \frac{x^2}{4} + \mu |\varphi|^{4/3} + g |\varphi|^2 \right] \varphi = 0, \quad (2.8)$$

where $g = 6\sqrt{2} N a_{12}/l$ and $\mu = 3(3\pi N/2)^{2/3}$ [40]. Here we have set the absorptive terms to zero for stationary states. We consider the following trial Gaussian wave function for

the solution of (2.8) [40]

$$\varphi(x, t) = A(t) \exp \left[-\frac{x^2}{2R^2(t)} + \frac{i}{2}\beta(t)x^2 + i\alpha(t) \right], \quad (2.9)$$

where $A(t)$, $R(t)$, $\beta(t)$, and $\alpha(t)$ are the normalization, width, chirp, and phase, respectively. The normalization condition $\int_0^\infty dx x^2 \varphi^2(x, t) = 1$ sets $A(t) = [\pi^{1/4} R^{3/2}(t)/2]^{-1}$. The Lagrangian density for generating (2.8) is [40]

$$\begin{aligned} \mathcal{L}(\varphi) &= \frac{i}{2} (\dot{\varphi}\varphi^* - \dot{\varphi}^*\varphi) - \left| \frac{\partial\varphi}{\partial x} \right|^2 - \frac{x^2}{4} |\varphi|^2 \\ &\quad - \frac{1}{2}g|\varphi|^4 - \frac{3}{5}\mu|\varphi|^{10/3}, \end{aligned} \quad (2.10)$$

where the overhead dot represents time derivative. The trial wave function (2.9) is substituted in the Lagrangian density and the effective Lagrangian L_{eff} is calculated via $L_{\text{eff}} = \int \mathcal{L}(\varphi) d^3x$:

$$\begin{aligned} L_{\text{eff}} &= \frac{\pi^{3/2} A^2(t) R^5(t)}{2} \left[-\frac{3}{2}\dot{\beta}(t) - \frac{g}{2\sqrt{2}} \frac{A^2(t)}{R^2(t)} \right. \\ &\quad \left. - \frac{9\sqrt{3}}{25\sqrt{5}} \mu \frac{A^{4/3}(t)}{R^2(t)} - \frac{2\dot{\alpha}(t)}{R^2(t)} - \frac{3}{R^4(t)} - 3\beta^2(t) - \frac{3}{4} \right]. \end{aligned} \quad (2.11)$$

The generalized Lagrange equations for this effective Lagrangian given by [38]

$$\frac{d}{dt} \frac{\partial L_{\text{eff}}}{\partial \dot{\gamma}(t)} = \frac{\partial L_{\text{eff}}}{\partial \gamma(t)}, \quad (2.12)$$

with $\gamma(t)$ representing $\alpha(t)$, $A(t)$, $\beta(t)$, and $R(t)$ are written explicitly as

$$\pi^{3/2} A^2 R^3 = \text{constant} = 4\pi, \quad (2.13)$$

$$3\dot{\beta} + \frac{4\dot{\alpha}}{R^2} + \frac{6}{R^4} + 6\beta^2 + \frac{3}{2} = -\frac{\sqrt{2}gA^2}{R^2} - \frac{6\sqrt{3}\mu A^{4/3}}{5\sqrt{5}R^2}, \quad (2.14)$$

$$\dot{R} = 2R\beta, \quad (2.15)$$

$$5\dot{\beta} + \frac{4\dot{\alpha}}{R^2} + \frac{2}{R^4} + 10\beta^2 + \frac{10}{4} = -\frac{gA^2}{\sqrt{2}R^2} - \frac{18\sqrt{3}\mu A^{4/3}}{25\sqrt{5}R^2}, \quad (2.16)$$

where the time dependence of different observable is suppressed. Eliminating α between (2.14) and (2.16) one obtains

$$2\dot{\beta} = \frac{4}{R^4} - 4\beta^2 + \frac{gA^2}{\sqrt{2}R^2} + \frac{12\sqrt{3}\mu A^{4/3}}{25\sqrt{5}R^2} - 1. \quad (2.17)$$

From (2.15) and (2.17) we get the following second-order differential equation for the evolution of the width R

$$\frac{d^2 R}{dt^2} = \frac{4}{R^3} + \frac{4g}{\sqrt{2}\pi R^4} + \frac{12\mu A^{2/3}\sqrt{3}}{25\pi^{1/3}\sqrt{5}R^3} - R, \quad (2.18)$$

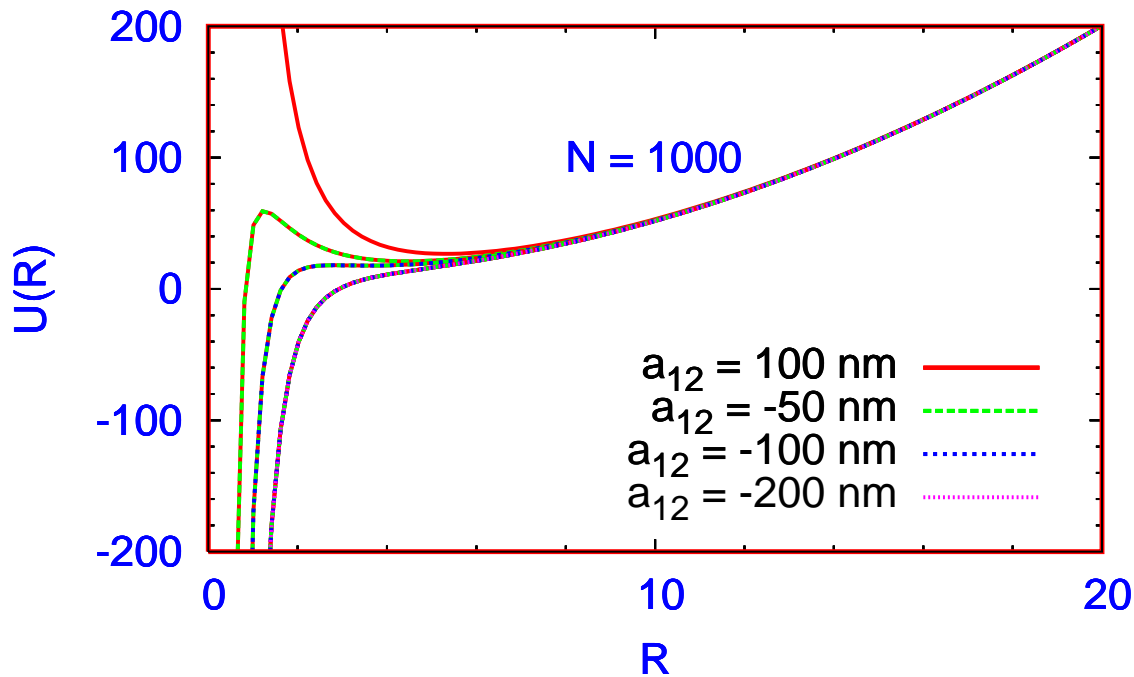


Figure 1. The effective potential $U(R)$ of (2.20) vs. R for different a_{12} and $N = 1000$ and $l = 1 \mu\text{m}$.

$$= -\frac{d}{dR} \left[\frac{2}{R^2} + \frac{4g}{3\sqrt{2\pi}} \frac{1}{R^3} + \frac{6\mu^{4^{2/3}}\sqrt{3}}{25\pi^{1/3}\sqrt{5}R^2} + \frac{R^2}{2} \right]. \quad (2.19)$$

The quantity in the square brackets of (2.19) is the effective potential $U(R)$ of the equation of motion:

$$U(R) = \frac{2}{R^2} + \frac{4g}{3\sqrt{2\pi}} \frac{1}{R^3} + \frac{6\mu^{4^{2/3}}\sqrt{3}}{25\pi^{1/3}\sqrt{5}R^2} + \frac{R^2}{2}. \quad (2.20)$$

Small oscillation of a stationary state around a stable configuration is possible when there is a minimum in this effective potential determined by a zero of (2.18). This condition yields the variational width from which the variational solution for the wave function is obtained via (2.9).

In figure 1 we plot the effective potential $U(R)$ of (2.20) for different a_{12} , $N = 1000$ and $l = 1 \mu\text{m}$. For positive (repulsive) $a_{12} = 100 \text{ nm}$, $U(R)$ leads to a confining well with a minimum at $R = R_0 = 5.3$, so that one could have a stable DFG of width $R_0 = 5.3$. The variational profile for this function is

$$\varphi(x) = \frac{2}{\pi^{1/4}R_0^{3/2}} \exp \left[-\frac{x^2}{2R_0^2} \right]. \quad (2.21)$$

In figure 1, as a_{12} turns gradually negative (attractive), the infinite wall near $R = 0$ of $U(R)$ is gradually lowered and for a sufficiently attractive scattering length $a_{12} \approx -100 \text{ nm}$, this wall disappears completely and one has the possibility of collapse for $a_{12} < -100 \text{ nm}$. The minimum in $U(R)$ first becomes a point of inflection for $a_{12} \approx -100 \text{ nm}$ and

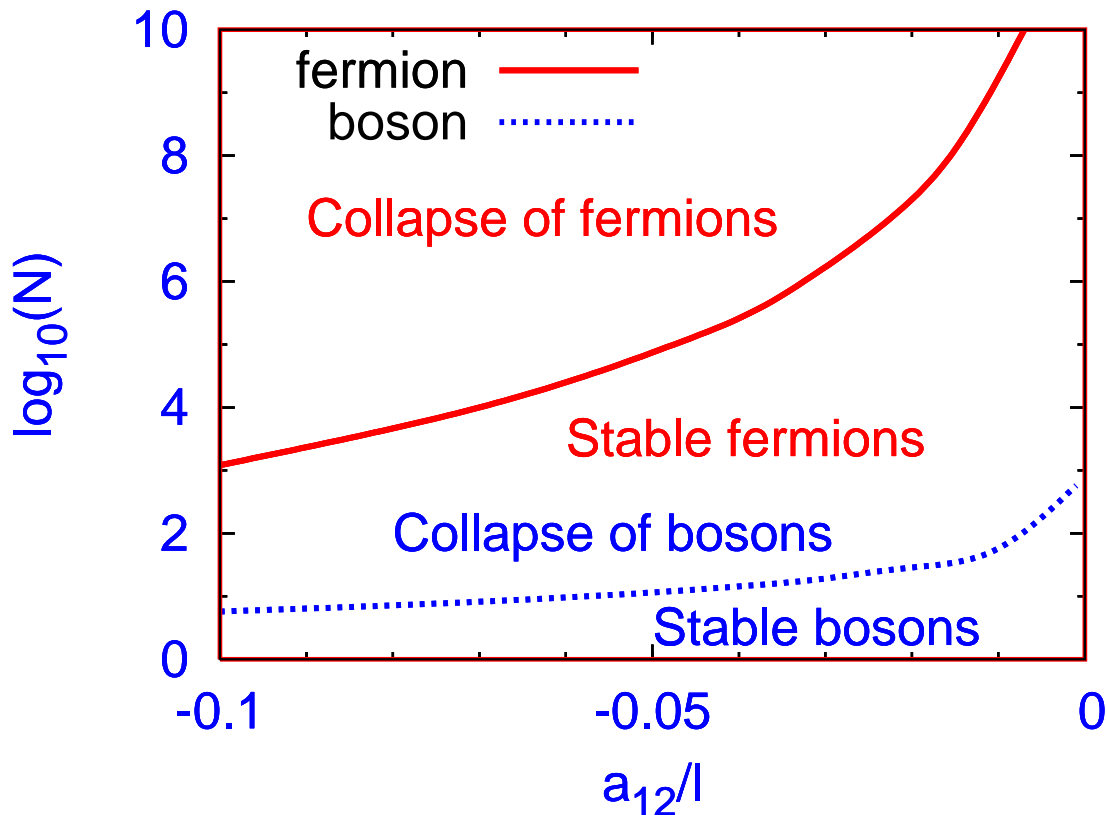


Figure 2. The phase diagram for collapse where we plot $\log_{10}(N)$ vs. a_{12}/l for fermion-fermion mixture (full line) and bosons (dotted line). The line separates the regions where collapse is present and absent.

then disappears. The profile of the effective potential in figure 1 is similar to the same in the bosonic case [33, 40].

Next we show the phase diagram for collapse for $N_1 = N_2 = N$ using the variational approach in figure 2, where we plot $\log_{10}(N)$ vs. a_{12}/l . The line separates the plot in two regions. In the upper half of the plot collapse is possible and in the lower half we have stable configurations. The phase diagram of figure 2 is quite similar to that obtained in Ref. [23] in a study of the stability of a DFFM. In case of bosons in a spherically-symmetric trap the line of stability is given by $Na/l = -0.575$ [33] and is also shown in figure 2. As expected, for a fixed $|a/l|$ a much larger number of fermions can be accommodated in a stable state.

3. Numerical Results

In this section we present results on collapse from a numerical solution of (2.6) and (2.7). After some experimentation we take in the initial DFFM $N_1 = 1000$, $N_2 = 2000$, and $a_{12} = 100$ nm, so that $a_{12}/l = 0.1$. This corresponds to nonlinearities $\mathcal{N}_{11} = 843$, $\mathcal{N}_{22} = 1338$, $\mathcal{N}_{12} = 200$ and $\mathcal{N}_{21} = 100$. The collapse dynamics is sensitive to the loss

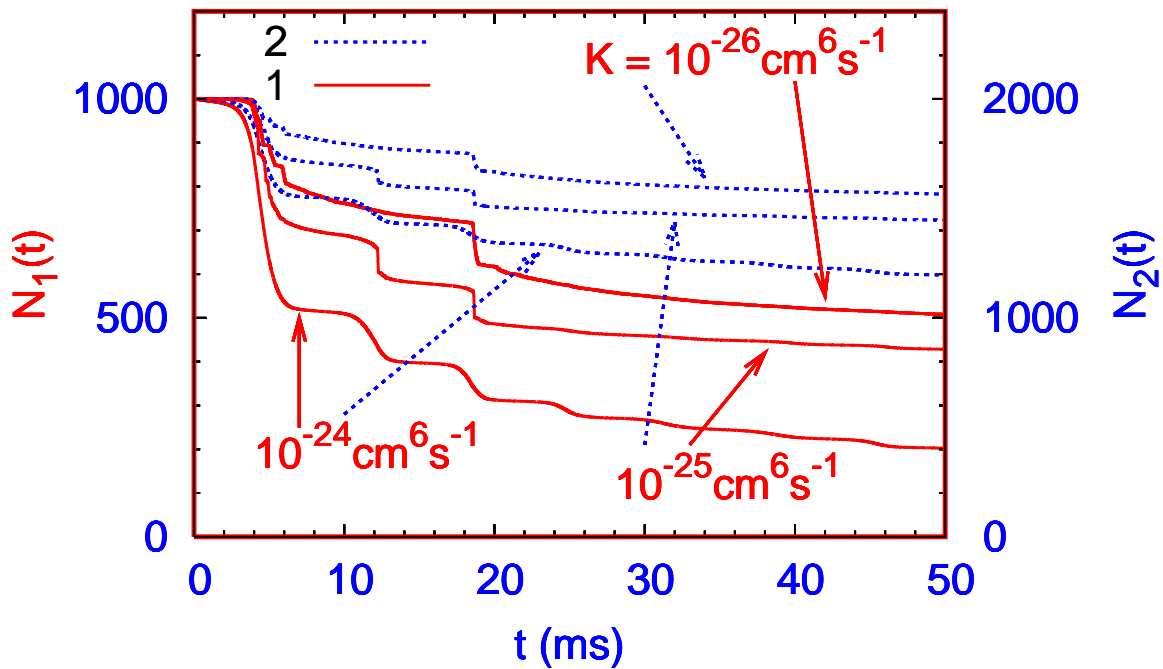


Figure 3. The evolution of fermion numbers $N_j(t)$ of the two components vs. time during a collapse initiated by a jump in scattering length a_{12} from 100 nm to -200 nm in a DFFM of $N_1 = 1000$ and $N_2 = 2000$ for three-body loss rates $K = 10^{-26} \text{ cm}^6 \text{ s}^{-1}$, $10^{-25} \text{ cm}^6 \text{ s}^{-1}$, and $10^{-24} \text{ cm}^6 \text{ s}^{-1}$. The dotted (blue) curves refer to fermion 2 and the solid (red) curves to fermion 1. The curves are labeled by their respective K values.

rates K_{31} and K_{32} . As these loss rates are not experimentally known, in the present simulation we take them to be equal: $K \equiv K_{31} = K_{32}$, and consider different values of K .

Now we consider the collapse of fermions initiated by a sudden jump in the fermion-fermion scattering length from $a_{12} = 100$ nm to -200 nm which can be implemented near a fermion-fermion Feshbach resonance, observed in fermionic systems [35]. This resonance should enable an experimental control of the interspecies interaction [17] and hence can be used to increase the attractive force between interspecies fermions by varying a background magnetic field, which in turn increases the attractive nonlinearities $6\sqrt{2}\mathcal{N}_{12}$ and $6\sqrt{2}\mathcal{N}_{21}$ in (2.6) and (2.7). If these attractive nonlinear terms can overcome the repulsive nonlinearities in these equations it is possible to have a collapse of fermions.

Due to the three-body loss terms in (2.6) and (2.7) the number of fermions decay with time. When the net nonlinear attraction in these equations is small there is a smooth and steady decay of number of atoms. However, when the net nonlinear attraction is jumped to a large value, the steady decay of number of atoms develops into a violent decay called collapse. When this happens, the DFFM loses a significant fraction of atoms in a small interval of time (milliseconds) after which a remnant DFG with a reasonably constant number of atoms is formed. Also, during and immediately

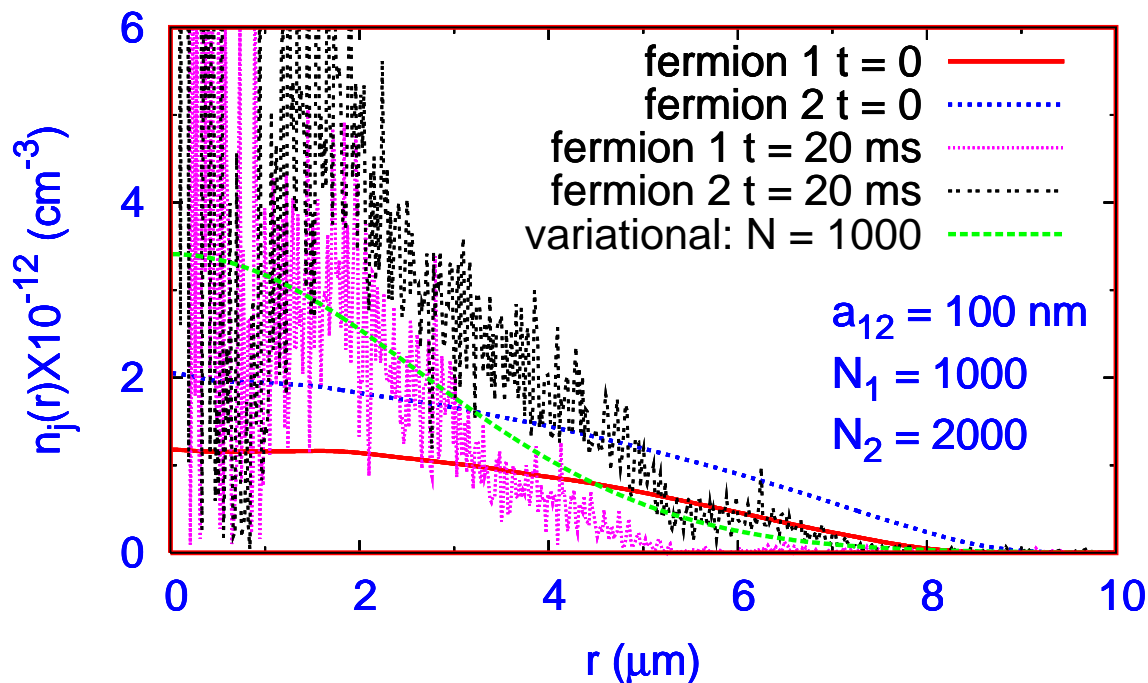


Figure 4. The fermion density $n_j(r)$ at $t = 0, 20$ ms before and during the collapse exhibited in figure 3 for $K = 10^{-26} \text{ cm}^6 \text{ s}^{-1}$. The density calculated from the variational profile of the wave function (2.21) for $R_0 = 5.3$ and $N = 1000$ is also shown,

after collapse, the fermion density function becomes unsmooth and spiky in nature as opposed to a reasonably smooth function in the case of a steady decay. This also happened in the collapse of a BEC [16].

We study the evolution of fermion numbers in the DFFM from time $t = 0$ to $t = 50$ ms after a sudden jump in the scattering length from $a_{12} = 100$ nm to -200 nm at $t = 0$. In agreement with the variational analysis of last section we find that this jump in the scattering length leads to collapse. The evolution of fermion numbers after the jump in scattering length a_{12} depends on the value of the three-body loss rate K . We study the sensitivity of the result on K by performing the calculation for different loss rates. In figure 3 we plot the evolution of the fermion numbers for loss rates: $K = 10^{-26} \text{ cm}^6 \text{ s}^{-1}$, $10^{-25} \text{ cm}^6 \text{ s}^{-1}$, and $10^{-24} \text{ cm}^6 \text{ s}^{-1}$. With the increase of K , the decay rate increases, although the results for different K are qualitatively similar. We see in figure 3 that, in all cases, the number of fermions decays rapidly and attain an approximately constant (remnant) value in less than 50 ms as in the case of bosons [16, 18]. We used a space step of 0.025 in the numerical solution of (2.6) and (2.7) and found that this step size was sufficient to reach a converged result even during collapse. In our previous study on the collapse of a BEC of ^{85}Rb [18, 20] we found that even a much larger step size of 0.1 led to converged result for the number of atoms in the remnant in quantitative agreement with experiment [16]. This gives assurance on the reliability of the present

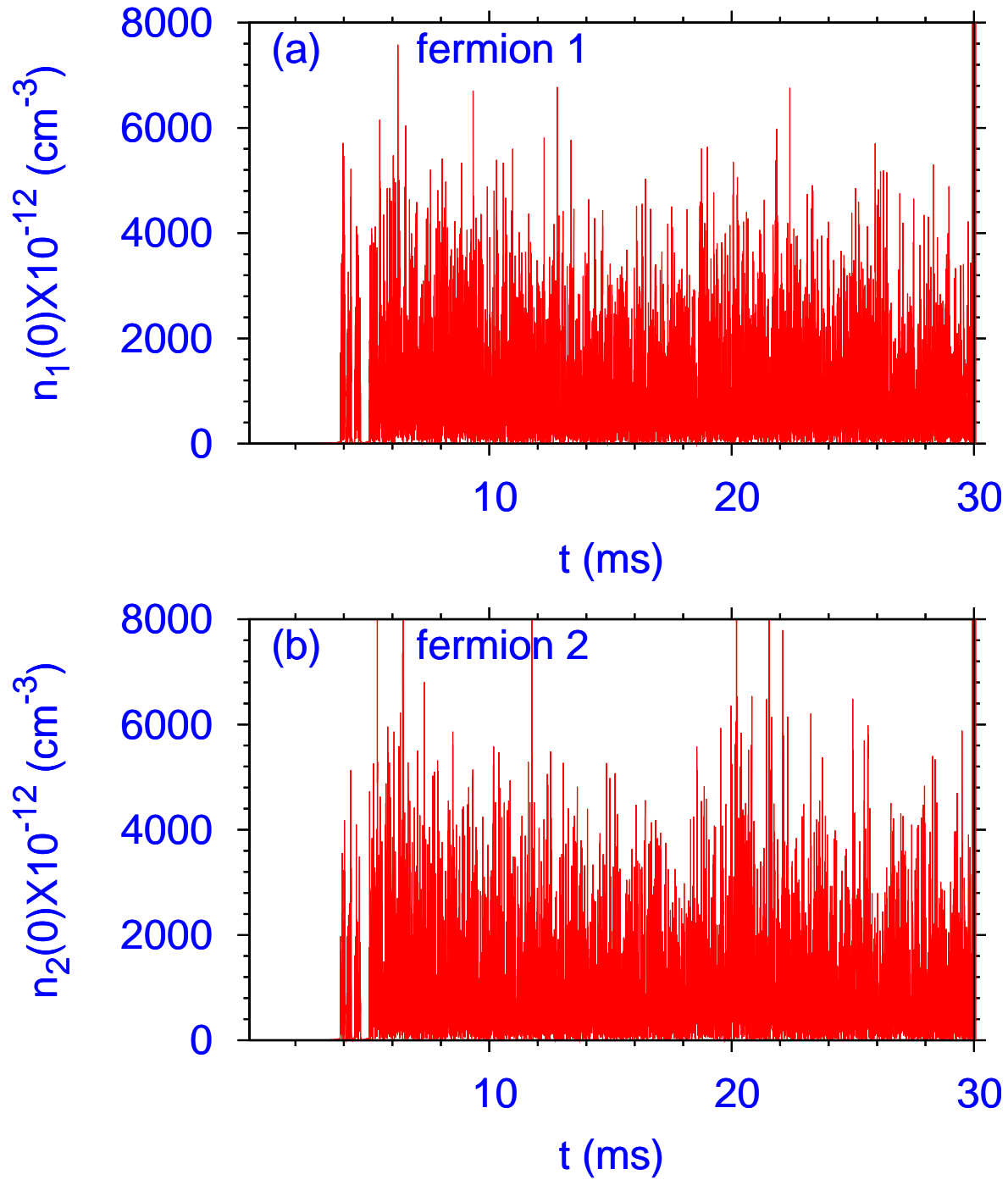


Figure 5. Evolution of central density $n_j(0)$ of fermion $j =$ (a) 1 and (b) 2 during the collapse exhibited in figure 3 for $K = 10^{-26} \text{ cm}^6\text{s}^{-1}$.

calculation.

In figure 4 we plot the fermion probability densities at times $t = 0$ and $t = 20$ ms. A close look at figure 4 reveals that before collapse at $t = 0$ the fermion densities are smooth. We have also plotted here the density corresponding to the variational profile

(2.21) for $R_0 = 5.3$ for fermion number $N = 1000$. Although the ranges of the exact and variational densities agree with each other, the functions do not agree well. This is understandable as the exact profile of the DFG is very different from the Gaussian trial function used in variational calculation. Although the fermion densities at $t = 0$ are smooth, the fermion densities during and after collapse have an entirely different profile. As expected the densities are highly peaked in the central ($r = 0$) region and develop spikes. Near $r = 0$ the densities could be two to three orders of magnitude larger than those for larger r values (see figure 5). However, they extend over a large distance too. The final spiky function indicates the collapse, in contrast to a smooth final function corresponding to a steady loss of atoms. The collapse is a quick process lasting at most a few tens of milliseconds when a significant fraction of atoms are lost. For example, in figure 3 for $K = 10^{-24} \text{ cm}^6\text{s}^{-1}$, the collapse lasts for the first 25 ms when most of the atoms are lost. After this interval the rate of loss of atoms is reduced and remnant a DFG with a roughly constant number of atoms are formed.

To confirm further the collapse in figures 3 and 4 for $K = 10^{-26} \text{ cm}^6\text{s}^{-1}$, we plot in figure 5 the evolution of the central probability density $n_j(0)$ of fermion j during collapse. We note a very strong fluctuation of a very large central density reminiscent of collapse in both components. The central density is three orders of magnitude larger than the equilibrium density in figure 4. Similar fluctuations were noted in the collapse of a pure BEC [19] as well as a DBFM [20]. Such a strong fluctuation of the central density could not be due to a weak evaporation of the DFFM due to recombination.

From figure 3 we find that the number of fermions remains practically constant during the first 4 ms or so after jumping the scattering length from 100 nm to -200 nm indicating that the collapse starts only after this interval of time. This is confirmed from the plot of central densities in figure 5 where we see that very large values of central density also appear after an interval of time called “time to collapse”. A similar phenomenon was also observed in the collapse of bosons [16]. Next we study an evolution of this time to collapse (t_{collapse}) with changing initial (a_{initial}) and final (a_{collapse}) scattering lengths. This is shown in figure 6 for two values of a_{initial} , where we plot t_{collapse} vs. a_{collapse} for $N_1 = 1000$, $N_2 = 2000$ and $K = 10^{-26} \text{ cm}^6\text{s}^{-1}$. The time to collapse is large for a small jump in the scattering length and reduces when the jump in the scattering length is increased, as also observed in the case of bosons [16].

One interesting aspect of figure 3 is the appearance of a revival of collapse. The fermion number after the primary collapse remains approximately constant for an interval of time and then again reduces abruptly. This revival of collapse takes place several times. A similar revival of collapse was noted in the fermion component in a numerical simulation in a DBFM [20] and was confirmed later in an experiment [11] on the ^{87}Rb - ^{40}K DBFM. To study the revival of collapse further in a DFFM we considered a different jump in the scattering length. For the same initial state of figure 3 we now consider a jump in a_{12} from 100 nm to -300 nm and the dynamics is reported in figure 7 for different K values. We find that the revival of collapse has practically disappeared in this case. If the collapse is initiated by a small jump in the scattering length, the

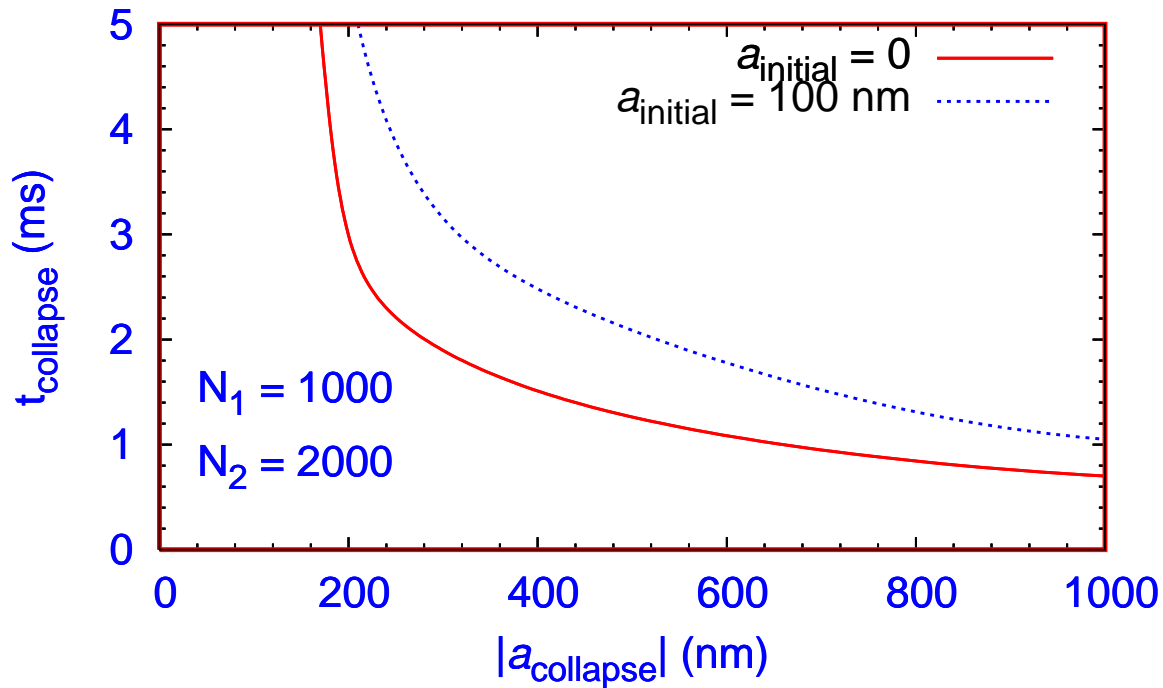


Figure 6. The evolution of time to collapse t_{collapse} vs. final scattering length a_{collapse} for $a_{\text{initial}} = 0$ and 100 nm for a DFFM with $N_1 = 1000$, $N_2 = 2000$ and $K = 10^{-26} \text{ cm}^6\text{s}^{-1}$. The curves are labeled by their respective a_{initial} values.

initial collapse is less violent. However, after this initial milder collapse the DFFM cannot reach an equilibrium state and it remains large and attractive. Consequently, the DFFM undergoes further collapse(s). On the other hand, if the collapse is initiated by a large jump in the scattering length, the initial collapse is very violent through which the DFFM gets rid of a very large number of atoms. Consequently, the DFFM reaches reasonably small and cold remnant states which do not further undergo collapse and one has one primary collapse. This is clear from figures 3 and 7. In figure 3 after the first collapse the DFFM loses a smaller percentage of atoms whereas in figure 7 a large percentage of atoms are lost after the primary collapse.

It was found in the experiment on collapse on a BEC [16] that during collapse the root mean square (rms) sizes of the condensate execute periodic oscillation with approximately twice the frequency of the trap. A breathing oscillation of same frequency was found in a BEC when a small perturbation was applied [34]. In dimensionless unit, the angular frequency of the trap is $\omega = 1$, corresponding to a (linear) frequency of $1/(2\pi)$. The observed frequency of oscillation of rms size was $1/\pi$ [16] – twice the trap frequency. In actual time unit the frequency of oscillation of rms sizes during collapse corresponds to $1/(2\pi) \text{ ms}^{-1} \approx 0.16 \text{ ms}^{-1}$. We also investigated if such oscillation existed in the present case in the DFFM during the collapse. In figure 8 we plot the rms radii of the two components of the collapsing DFFM and find that they also execute quasi-periodic oscillation. The calculated frequency from figure 8 is 0.145 ms^{-1} close to that

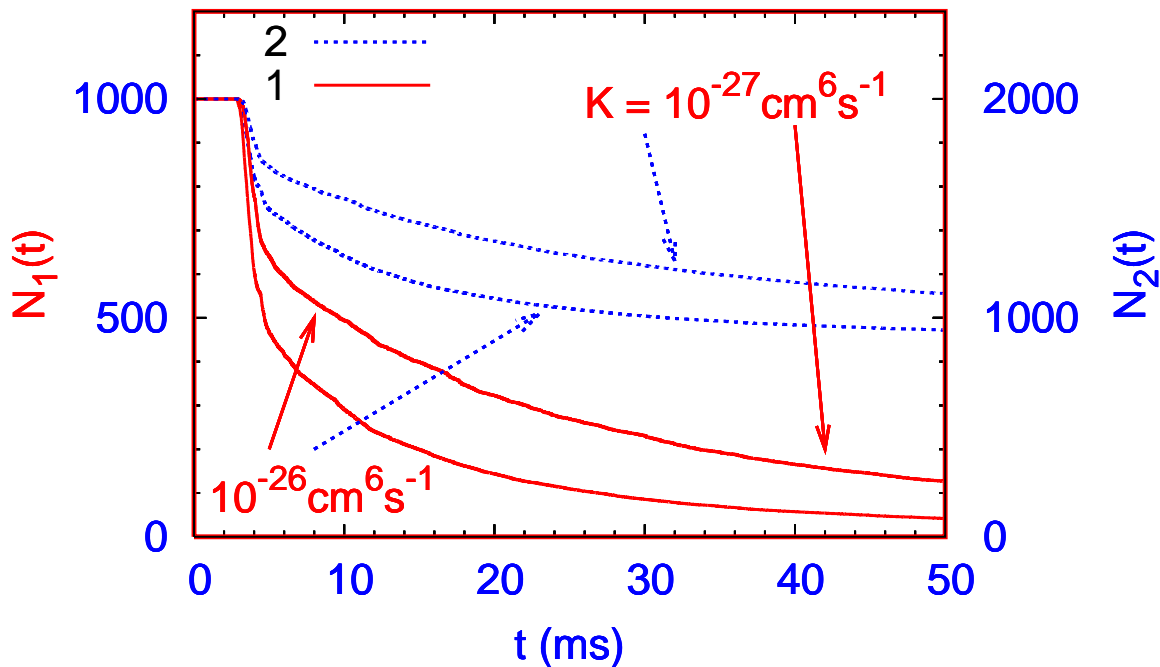


Figure 7. The evolution of fermion numbers $N_j(t)$ during collapse initiated by a jump in scattering length a_{12} from 100 nm to -300 nm for $K = 10^{-27} \text{ cm}^6 \text{ s}^{-1}$, $10^{-26} \text{ cm}^6 \text{ s}^{-1}$, and $10^{-25} \text{ cm}^6 \text{ s}^{-1}$. The dotted (blue) curves refer to fermion 2 and the solid (red) curves to fermion 1. The curves are labeled by their respective K values.

found in the case of bosons, e.g. 0.16 ms^{-1} . The difference could be due to the coupled nature of the hydrodynamic equations as well as the very large nonlinearity for fermions.

4. Summary

We suggested a coupled set of time-dependent hydrodynamic equations for a trapped DFFM including the effect of three-body recombination. The present time-dependent formulation permits us to study the non-equilibrium dynamics of a DFFM. Using a variational analysis as well as a numerical solution of our model, we study, for an attractive inter-species fermion-fermion interaction, the collapse in a DFFM composed of two types of nonidentical atoms. The collapse of a DFFM of two different atoms can be realized experimentally by jumping the inter-species scattering length to a large negative value by exploiting a fermion-fermion Feshbach resonance [35]. The collapse dynamics is strongly dependent on the three-body loss rate K and we present results for different loss rates. We note the possibility of a revival of collapse in a DFFM as in a previous simulation [20] on a DBFM, confirmed later in an experiment [11] on ^{87}Rb - ^{40}K . We find that a revival of collapse in a DFFM takes place for a moderate jump in the interspecies scattering length which disappears for a larger jump. We also study the quasi-periodic oscillation of the DFFM with approximately twice the trap frequency

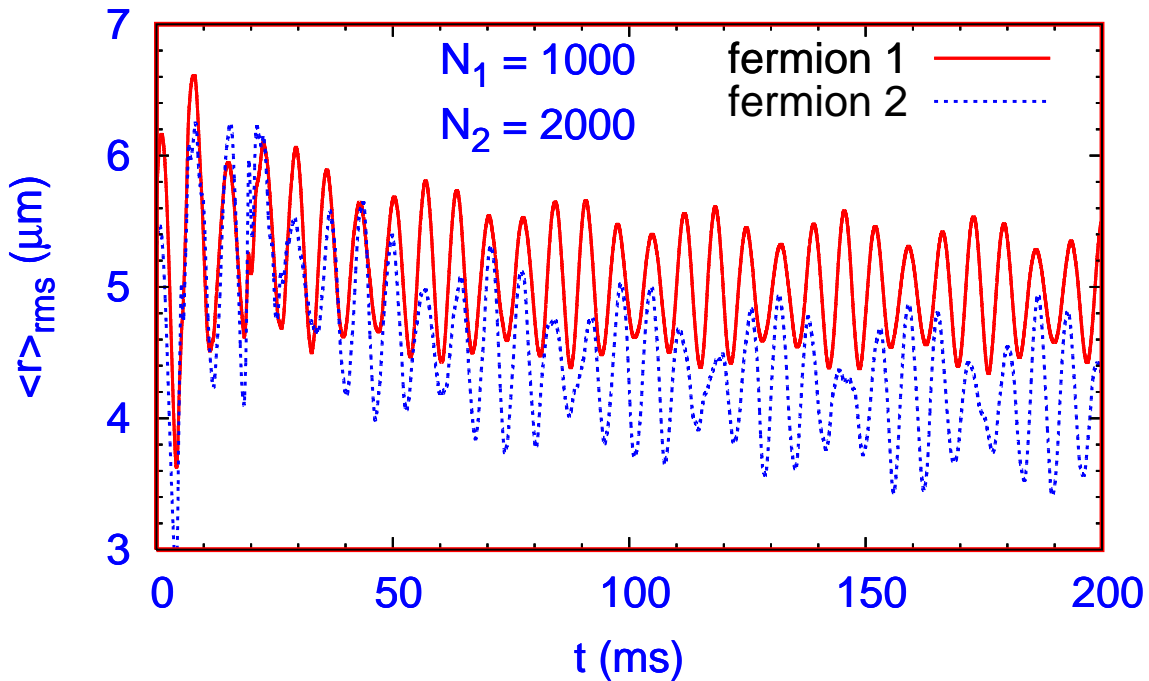


Figure 8. The rms radii of the two components vs. time before and during collapse exhibited in figure 3 for $N_1 = 1000$ and $N_2 = 2000$ initiated by a jump in scattering length a_{12} from 100 nm to -200 nm for $K = 10^{-26} \text{ cm}^6\text{s}^{-1}$. The dotted (blue) curves refer to fermion 2 and the solid (red) curves to fermion 1.

during collapse and explosion.

A proper treatment of a DFFM should be performed using a fully antisymmetrized many-body Slater determinant wave function [41] as in the case of atomic and molecular scattering involving many electrons [42]. However, in view of the success of the hydrodynamic model in a description of a collapse [20], the formation of bright [27] and dark [28] solitons, and vortex states [32] in a DBFM, we do not believe that the present study on the collapse in a DFFM to be so peculiar as to have no general validity. The present study on collapse in a DFFM of nonidentical atoms can be verified in future experiments, which can really validate the present hydrodynamic model and the related numerical study.

Acknowledgments

The work is supported in part by the CNPq and FAPESP of Brazil.

References

- [1] DeMarco B and Jin D S 1999 *Science* **285** 1703
- [2] O'Hara K M, Hemmer S L, Gehm M E, Granade S R and Thomas J E 2002 *Science* **298** 2179

- [3] Jochim S, Bartenstein M, Hendl G, Denschlag J H, Grimm R, Mosk A and Weidemuller M 2002 *Phys. Rev. Lett.* **89** 273202
Jochim S, Bartenstein M, Altmeyer A, Hendl G, Chin C, Denschlag J H and Grimm R 2003 *Phys. Rev. Lett.* **91** 240402
- [4] Chin C, Bartenstein M, Altmeyer A, Riedl S, Jochim S, Denschlag J H and Grimm R 2004 *Science* **305** 1128
Partridge G B, Li W H, Kamar R I, Liao Y A and Hulet R G 2006 *Science* **311** 503
- [5] Houbiers M, Ferwerda R, Stoof H T C, McAlexander W I, Sackett C A and Hulet R G 1997 *Phys. Rev. A* **56** 4864
- [6] Schreck F, Khaykovich L, Corwin K L, Ferrari G, Bourdel T, Cubizolles J and Salomon C 2001 *Phys. Rev. Lett.* **87** 080403
Truscott A G, Strecker K E, McAlexander W I, Partridge G B and Hulet R G 2001 *Science* **291** 2570
- [7] Hadzibabic Z, Stan C A, Dieckmann K, Gupta S, Zwierlein M W, Gorlitz A and Ketterle W 2002 *Phys. Rev. Lett.* **88** 160401
- [8] Strecker K E, Partridge G B and Hulet R G 2003 *Phys. Rev. Lett.* **91** 080406
Hadzibabic Z, Gupta S, Stan C A, Schunck C H, Zwierlein M W, Dieckmann K and Ketterle W 2003 *Phys. Rev. Lett.* **91** 160401
- [9] Modugno G, Roati G, Riboli F, Ferlaino F, Brecha R J and Inguscio M 2002 *Science* **297** 2240
- [10] Roati G, Riboli F, Modugno G and Inguscio M 2002 *Phys. Rev. Lett.* **89** 150403
- [11] Ospelkaus C, Ospelkaus S, Sengstock K and Bongs K 2006 *Phys. Rev. Lett.* **96** 020401
- [12] Gunter K, Stoferle T, Moritz H, Kohl M and Esslinger T 2006 *Phys. Rev. Lett.* **96** 180402
Goldwin J, Papp S B, DeMarco B and Jin D S 2002 *Phys. Rev. A* **65** 021402
- [13] Zwierlein M W, Abo-Shaeer J R, Schirotzek A, Schunck C H and Ketterle W 2005 *Nature* **435** 1047
Zwierlein M W, Schirotzek A, Schunck C H and Ketterle W 2006 *Science* **311** 492
- [14] Zaccanti M, D'Errico C, Ferlaino F, Roati G, Inguscio M and Modugno G 2006 "Control of the interaction in a Fermi-Bose mixture" cond-mat/0606757
Ospelkaus S, Ospelkaus C, Humbert L, Sengstock K and Bongs K 2006 *Phys. Rev. Lett.* **97** 120403
- [15] Gerton J M, Strelakov D, Prodan I and Hulet R G 2001 *Nature* **408** 692
- [16] Donley E A, Claussen N R, Cornish S L, Roberts J L, Cornell E A and Wieman C E 2001 *Nature* **412** 295
- [17] Inouye S, Andrews M R, Stenger J, Miesner H J, Stamper-Kurn D M and Ketterle W 1998 *Nature* **392** 151
- [18] Adhikari S K 2002 *Phys. Rev. A* **66** 043601
Adhikari S K 2005 *Phys. Rev. A* **71** 053603
- [19] Santos L and Shlyapnikov G V 2002 *Phys. Rev. A* **66** 011602(R)
Saito H and Ueda M 2002 *Phys. Rev. A* **65** 033624
Savage C M, Robins N P and Hope J J 2003 *Phys. Rev. A* **67** 014304
Duine R A and Stoof H T C 2003 *Phys. Rev. A* **68** 013602
Calzetta E A and Hu B L 2003 *Phys. Rev. A* **68** 043625
Bao W, Jaksch D and Markowich P A 2004 *J. Phys. B: At. Mol. Opt. Phys.* **37** 329
Adhikari S K 2004 *J. Phys. B: At. Mol. Opt. Phys.* **37** 1185
- [20] Adhikari S K 2004 *Phys. Rev. A* **70** 043617
- [21] Modugno M, Ferlaino F, Riboli F, Roati G, Modugno G and Inguscio M 2003 *Phys. Rev. A* **68** 043626
- [22] Gehm M E, Hemmer S L, Granade S R, O'Hara K M and Thomas J E 2003 *Phys. Rev. A* **68** 011401(R)
- [23] Roth R and Feldmeier H 2001 *J. Phys. B: At. Mol. Opt. Phys.* **34** 4629
- [24] Kokkelmans S J J M F, Milstein J N, Chiofalo M L, Walser R and Holland M J 2002 *Phys. Rev.*

A **65** 053617

- [25] Heiselberg H 2001 *Phys. Rev. A* **63** 043606
- [26] Hulet R G 2006 private communication. I thank Dr. Hulet for a discussion, which clarified this point, suggesting the strong possibility of collapse in a DFFM of different atoms.
- [27] Adhikari S K 2005 *Phys. Rev. A* **72** 053608
- [28] Adhikari S K 2005 *J. Phys. B: At. Mol. Opt. Phys.* **38** 3607
- [29] Adhikari S K 2006 *Phys. Rev. A* **73** 043619
- [30] Adhikari S K 2006 *Laser Phys. Lett.* in press
Adhikari S K 2006 *Laser Phys. Lett.* in press
- [31] Karpiuk T, Brewczyk M, Ospelkaus-Schwarzer S, Bongs K, Gajda M and Rzążewski K 2004 *Phys. Rev. Lett.* **93** 100401
- [32] Jezek D M, Barranco M, Guilleumas M, Mayol R and Pi M 2004 *Phys. Rev. A* **70** 043630
Guilleumas M, Centelles M, Barranco M, Mayol R and Pi M 2005 *Phys. Rev. A* **72** 053602
- [33] Dalfovo F, Giorgini S, Pitaevskii L P and Stringari S 1999 *Rev. Mod. Phys.* **71** 463
Yukalov V I 2004 *Laser Phys. Lett.* **1** 435
- [34] Adhikari S K and Muruganandam P 2002 *J. Phys. B: At. Mol. Opt. Phys.* **35** 2831
- [35] O'Hara K M, Hemmer S L, Granade S R, Gehm M E, Thomas J E, Venturi V, Tiesinga E and Williams C J 2002 *Phys. Rev. A* **66** 041401(R)
Dieckmann K, Stan C A, Gupta S, Hadzibabic Z, Schunck C H and Ketterle W 2002 *Phys. Rev. Lett.* **89** 203201
Loftus T, Regal C A, Ticknor C, Bohn J L and Jin D S 2002 *Phys. Rev. Lett.* **88** 173201
Regal C A, Greiner M and Jin D S 2004 *Phys. Rev. Lett.* **92** 083201
- [36] Adhikari S K 2001 *Phys. Rev. A* **63** 043611
Adhikari S K 2001 *J. Phys. B: At. Mol. Opt. Phys.* **34** 4231
- [37] Capuzzi P, Minguzzi A and Tosi M P 2003 *Phys. Rev. A* **67** 053605
Capuzzi P, Minguzzi A and Tosi M P 2003 *Phys. Rev. A* **68** 033605
- [38] Goldstein H 1980 *Classical Mechanics*, (Reading, Addison Wesley)
- [39] Muruganandam P and Adhikari S K 2003 *J. Phys. B: At. Mol. Opt. Phys.* **36** 2501
- [40] Pérez-García V M, Michinel H, Cirac J I, Lewenstein M and Zoller P 1996 *Phys. Rev. Lett.* **77** 5320
Stoof H T C 1997 *J. Stat. Phys.* **87** 1353
Adhikari S K 2005 *J. Phys. B: At. Mol. Opt. Phys.* **38** 579
Anderson D 1983 *Phys. Rev. A* **27** 3135
- [41] Molmer K 1998 *Phys. Rev. Lett.* **80** 1804
Liu X-J and Hu H 2003 *Phys. Rev. A* **67** 023613
Roth R and Feldmeier H 2002 *Phys. Rev. A* **65** 021603R
Miyakawa T, Suzuki T and Yabu H 2001 *Phys. Rev. A* **64** 033611
- [42] Biswas P K and Adhikari S K 2000 *J. Phys. B: At. Mol. Opt. Phys.* **33** 1575
Biswas P K and Adhikari S K 1998 *J. Phys. B: At. Mol. Opt. Phys.* **31** L315
Adhikari S K 1979 *Phys. Rev. C* **19** 1729
Adhikari S K and Ghosh A 1997 *J. Phys. A: Math. Gen.* **30** 6553
Tomio L and Adhikari S K 1980 *Phys. Rev. C* **22** 28